Title

In Vitro Magnetic Resonance Imaging Evaluation of Fragmented, Open-Coil, Percutaneous Peripheral Nerve Stimulation Leads

Journal

Neuromodulation Technology at the Neural Interface, 21(3)

ISSN

1094-7159

Authors

Shellock, Frank G
Zare, Armaan
Ilfeld, Brian M
et al.

Publication Date

2018-04-01

DOI

10.1111/ner.12705

Peer reviewed

Received: June 20, 2017 Revised: September 3, 2017 Accepted: September 6, 2017

(onlinelibrary.wiley.com) DOI: 10.1111/ner.12705

In Vitro Magnetic Resonance Imaging Evaluation of Fragmented, Open-Coil, Percutaneous Peripheral Nerve Stimulation Leads

Frank G. Shellock, PhD*; Armaan Zare†; Brian M. Ilfeld, MD, MS‡; John Chae, MD, ME§; Robert B. Strother¶

Objective: Percutaneous peripheral nerve stimulation (PNS) is an FDA-cleared pain treatment. Occasionally, fragments of the lead (MicroLead, SPR Therapeutics, LLC, Cleveland, OH, USA) may be retained following lead removal. Since the lead is metallic, there are associated magnetic resonance imaging (MRI) risks. Therefore, the objective of this investigation was to evaluate MRI-related issues (i.e., magnetic field interactions, heating, and artifacts) for various lead fragments.

Methods: Testing was conducted using standardized techniques on lead fragments of different lengths (i.e., 50, 75, and 100% of maximum possible fragment length of 12.7 cm) to determine MRI-related problems. Magnetic field interactions (i.e., translational attraction and torque) and artifacts were tested for the longest lead fragment at 3 Tesla. MRI-related heating was evaluated at 1.5 Tesla/64 MHz and 3 Tesla/128 MHz with each lead fragment placed in a gelled-saline filled phantom. Temperatures were recorded on the lead fragments while using relatively high RF power levels. Artifacts were evaluated using T1-weighted, spin echo, and gradient echo (GRE) pulse sequences.

Results: The longest lead fragment produced only minor magnetic field interactions. For the lead fragments evaluated, physiologically inconsequential MRI-related heating occurred at 1.5 Tesla/64 MHz while under certain 3 Tesla/128 MHz conditions, excessive temperature elevations may occur. Artifacts extended approximately 7 mm from the lead fragment on the GRE pulse sequence, suggesting that anatomy located at a position greater than this distance may be visualized on MRI.

Conclusions: MRI may be performed safely in patients with retained lead fragments at 1.5 Tesla using the specific conditions of this study (i.e., MR Conditional). Due to possible excessive temperature rises at 3 Tesla, performing MRI at that field strength is currently inadvisable.

Keywords: Artifacts, implants, magnetic resonance imaging, MRI, MRI safety, peripheral nerve stimulation

Conflict of Interest: Frank G. Shellock, PhD is a paid consultant for SPR Therapeutics, LLC. Armaan Zare has no potential conflicts of interest. Brian M. Ilfeld, MD, MS has received research funding from SPR Therapeutics, LLC. John Chae, MD, ME is the Chief Medical Advisor, SPR Therapeutics and owns equity in SPR Therapeutics, LLC. Robert Strother is the Chief Engineer of SPR Therapeutics, LLC and owns equity in SPR Therapeutics, LLC.

Address correspondence to: Frank G. Shellock, PhD, Departments of Radiology and Medicine, University of Southern California, 7751 Veragua Dr., Los Angeles, CA, 90293, USA. Email: frank.shellock@gte.net

* Departments of Radiology and Medicine, Keck School of Medicine, University of Southern California, Los Angeles, CA, USA;
† Loyola Marymount University, Los Angeles, CA, USA;
‡ Department of Anesthesiology, University of California San Diego, San Diego, San Diego, CA, USA;
§ Department of Physical Medicine and Rehabilitation, Case Western Reserve University, Cleveland, OH, USA; and
¶ SPR Therapeutics, LLC, Cleveland, OH, USA

For more information on author guidelines, an explanation of our peer review process, and conflict of interest informed consent policies, please go to http://www.wiley.com/WileyCDA/Section/id-301854.html

Source(s) of financial support: Research reported in this publication was supported, in part, by the Eunice Kennedy Shriver National Institute of Child Health and Human Development, Award Number R44HD067094; National Institute on Aging, Award Number R44AG052196; and the Department of Defense Peer Reviewed Orthopaedic Research Program, Award Number OR110066. The content of this article is solely the responsibility of the authors and does not necessarily represent the official views of the funding entities.

INTRODUCTION

Opioid addiction and misuse has become an epidemic in the United States and, therefore, safe and effective non-opioid pain management therapies are urgently needed. Neurostimulation, such as traditional methods of spinal cord stimulation (SCS) and peripheral nerve stimulation (PNS), may be used to reduce pain and has been reported to decrease or limit opioid use (1–8). However, these modalities typically require implantation of permanent stimulation devices through invasive surgery. As a result, neurostimulation using permanent components is often one of the last options in the treatment continuum for pain.

Recently, a percutaneous PNS system received Food and Drug Administration clearance for use in the back and/or extremities for the treatment of chronic and acute pain, including postoperative and posttraumatic pain. Clinical applications for percutaneous PNS have been investigated for the treatment of multiple types of pain, including low back pain, neuropathic pain following amputation, chronic shoulder pain, and postoperative pain following total knee replacement (1,2,9–20). This unique system consists of an external pulse generator connected to a percutaneously inserted, open-coil lead that is placed through a minimally invasive procedure and left indwelling for up to 30 days. At the completion of therapy, the lead is withdrawn. Thus, this percutaneous PNS strategy avoids the invasive surgical procedures required with traditional neurostimulation systems to implant permanent stimulation systems with multiple components (i.e., pulse generator, lead extension, and lead).

Occasionally, small lead fragments (typical length range, 5–25 mm) may be retained following lead removal. Because of the presence of this metallic lead fragment, there may be serious risks relative to the use of magnetic resonance imaging (MRI) (21–24). Therefore, the goal of this investigation was to use *in vitro* test methods to evaluate MRI-related issues (magnetic field interactions, MRI-related heating, and artifacts) for lead fragments of various lengths that may be present in patients referred for MRI.

MATERIALS AND METHODS

Open-Coil Lead Used for Percutaneous PNS

This investigation evaluated MRI issues for lead fragments associated with the SPRINT Peripheral Nerve Stimulation (PNS) System (SPR Therapeutics, LLC, Cleveland, OH, USA) (Fig. 1). The percutaneous PNS system consists of a lead connected via cables to a body-worn external pulse generator (Fig. 1). The intact lead and external components of the system are not intended for use in a patient undergoing an MRI examination and can be removed prior to undergoing an MRI. Therefore, they were not included in the MRI testing performed in this study. This evaluation of MRI issues only applies to any lead fragments retained in body tissue after the lead has been removed.

The lead utilized with this system (MicroLead, SPR Therapeutics, LLC, Cleveland, OH, USA) is a coiled, fine-wire that permits the electrode to be placed in tissue to deliver short-term electrical stimulation therapy to a peripheral nerve (i.e., FDA clearance for up to 60 days). The lead is composed of 7-strands of non-ferromagnetic 316L stainless steel, and each strand is 34 μm in diameter (0.00135 inch). Almost the entire length (12.7 cm) of the 7-strand wire is insulated by perfluoroalkoxy, PFA (poly fluorocarbon). The only portion of the lead that is uninsulated is a closely wound wire at the distal tip. The tip consists of 15 mm of the 7-strand stainless steel wire and close-wound on a 101 μm (0.004 inch) arbor. The terminal end of the tip (5 mm) is bent at an acute angle forming an anchor designed to resist lead migration (Fig. 2).

The lead fragments that were investigated in this study were constructed to provide representative examples that may pose MRI-related problems. In clinical use, the lead is preloaded within a 20 gauge, 12.7 cm (5.00 inch) introducer needle, which is placed into the target tissue using a percutaneous insertion procedure. Notably, the needle is not typically inserted completely into the tissue to reach the peripheral nerve, and the lead cannot be inserted beyond the tip of the needle due to the flexibility of the lead. Thus, the maximum possible length of the lead under the skin is 12.7 cm. In consideration of the coiling of the wire, a maximum 12.7 cm length of coiled lead that can be under the skin has a 37.6 cm length of insulated wire and a 9.5 cm length of uninsulated wire, close-wound and touching collapsed onto a 1 cm straight length, and a 0.5 cm anchor (i.e., a total of 47.1 cm of 7-strand stainless steel wire which is an electrical straight wire length of 39.1 cm). Thus, the aforementioned lengths were taken into consideration to select the fragmented lengths of the leads that underwent testing.

While visual examination of over 100 leads removed following pain management therapy revealed that a majority of leads are removed intact, the leads that fracture upon removal usually fracture at or near the distal tip ($\leq$15 mm), indicating that the 12.7 cm longest possible lead fragment that may be retained in the patient is very rare. Also, for some of the removed leads, lengths of the PFA insulating coating were broken, resulting in uninsulated areas at the end with the break. This resulted in an uninsulated length of wire (frequently $<$3 cm in length). Although it is most likely that this stretching, breaking and sliding of the PFA coating down the lead happened during the removal process, it remains a possibility that the portion of the lead retained in the tissue has a section of uninsulated wire (Fig. 3).

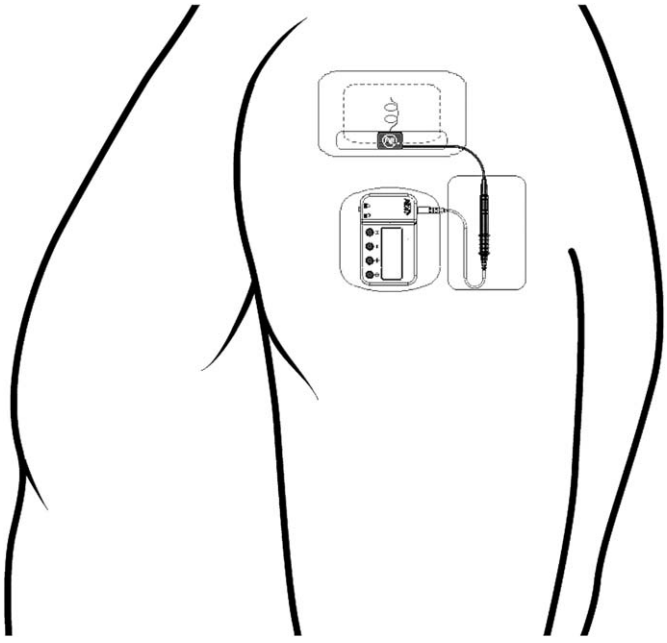

Figure 1. Body-worn percutaneous peripheral nerve stimulation system used for the treatment of chronic pain and acute pain, including postoperative and posttraumatic pain. This example shows application for management of chronic shoulder pain. Image used with permission from SPR Therapeutics.

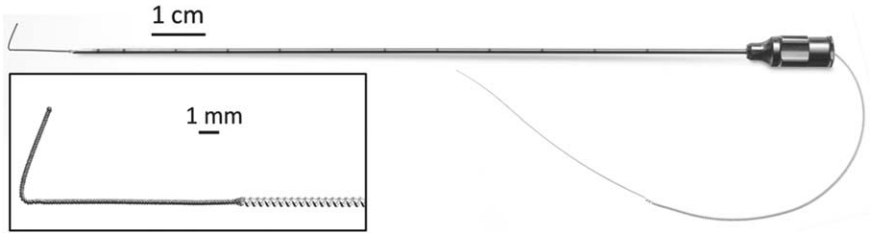

Figure 2. Open-coil lead used for percutaneous peripheral nerve stimulation, loaded into introducer needle. Inset: The 7-strand stainless steel wire is insulated except for the distal tip, which terminates in an anchor to secure the lead within tissue and prevent lead migration. Image used with permission from SPR Therapeutics.

Magnetic Field Interactions

Testing for magnetic field interactions involved evaluations of translational attraction and torque for the lead fragment, 12.7 cm length with the proximal 2 mm, uninsulated, using a 3 Tesla MR system (Fig. 3, bottom), following standard techniques (22–26).

Translational Attraction

For the assessment of translational attraction, a test was conducted known as the deflection angle test, as previously described (22–26). The lead fragment was attached to a special non-metallic, test apparatus to measure the deflection angle in the 3 Tesla MR system. The test fixture consisted of a structure steadily holding the lead fragment in position and incorporated a protractor with 1°-graduated markings, rigidly mounted to the structure (22–26). The 0° indicator on the protractor was oriented perpendicular. The test fixture also had a plastic bubble level attached to the top to ensure proper orientation and leveling in the MR system during the test procedure. Sources of forced air movement within the bore of the scanner were turned off during the measurements. The lead fragment was suspended from a thin, lightweight string (weight, less than 1% of the weight of the lead) that was attached to the protractor. Motion of the string with the lead fragment was not constrained by the support structure of the protractor.

Measurements of deflection angles for the lead were obtained in the MR system at the point of the highest, "patient accessible" (i.e., the position of which the patient would pass through while entering the bore of the MR system), spatial gradient magnetic field (22–33). This position was assessed using a gauss meter (Extech Model 480823, Electromagnetic Field Meter; Extech, Nashua, NH, USA). The value of the static magnetic field at the position where the translational attraction was determined for the lead was 1.53 Tesla and the spatial gradient magnetic field was 466 gauss/cm. The deflection angle for the lead from the vertical direction to the nearest 1° was measured three times and a mean value was calculated (22–33).

Qualitative Assessment of Torque

The next evaluation of magnetic field interactions was conducted to qualitatively determine the presence of magnetic field-induced torque for the lead fragment using a standardized test, as previously described (22–26,28–33). This procedure involved the use of a flat plastic material (low coefficient of friction) with a millimeter grid. The lead fragment was placed on the test apparatus in an orientation that was 45° relative to the static magnetic field of the 3 Tesla MR system. The test apparatus with the lead fragment was positioned in the center of the MR system, where the effect of torque from the static magnetic field is known to be the greatest (i.e., based on a previous magnetic field survey and the well-known characteristics of the 3 Tesla MR system with a horizontal magnetic field used for this evaluation) (22–26,28–33). The lead fragment was directly observed for possible movement with respect to alignment or rotation relative to the static magnetic field of the scanner. Having the investigator inside the bore of the MR system during the test procedure facilitated the observation process. The lead was moved 45° relative to its previous position and again observed for alignment or rotation (22–26,28–33). This process was repeated to encompass a full 360° rotation of positions for the lead fragment in the 3 Tesla MR system. The entire procedure was conducted three times and a mean value was calculated for the lead fragment with it orientated along both its long axis (22–26,28–33).

The following qualitative scale of torque was applied to the results: 0, no torque; +1, mild or low torque, the device slightly changed orientation but did not align to the magnetic field; +2, moderate torque, the device aligned gradually to the magnetic field;

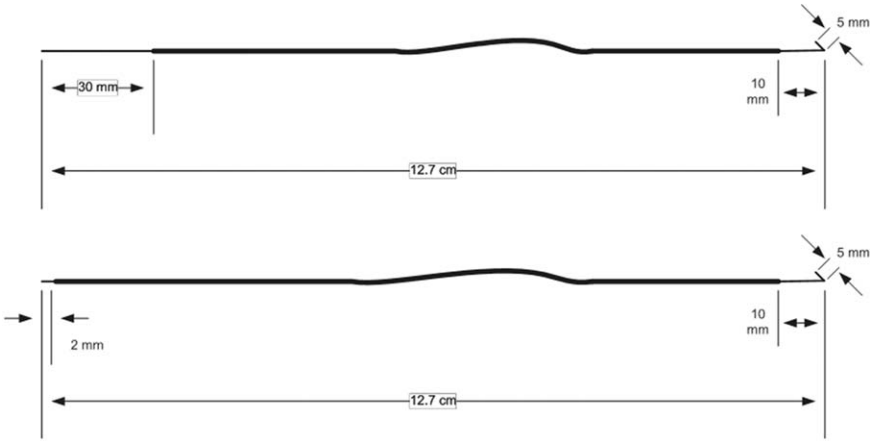

Figure 3. Schematic illustrating two 12.7 cm length test samples with 30 mm (top) and 2 mm (bottom) of uninsulated proximal tips.

Table 1. Summary of Temperature Rises for Fragmented Leads Evaluated for MRI-Related Heating at 1.5 Tesla/64 MHz and 3 Tesla/128 MHz.

Sample	MRI condition	Fragment length (cm) (% of maximum fragment length)	Proximal uninsulated length (cm)	Highest temperature rise tip (°C)	Highest temperature rise uninsulated end (°C)
1	1.5 Tesla/64 MHz	12.7 (100%)	3.0	2.8	3.1
2	1.5 Tesla/64 MHz	12.7 (100%)	0.2	3.3	3.5
3	3 Tesla/128 MHz	12.7 (100%)	3.0	3.6	4.5
4	3 Tesla/128 MHz	12.7 (100%)	0.2	3.8	4.8
5	3 Tesla/128 MHz	12.7 (100%)	0.2	4.4	5.2
6	3 Tesla/128 MHz	12.0 (94%)	0.2	5.8	5.9
7	3 Tesla/128 MHz	11.2 (88%)	0.2	3.5	3.7
8	3 Tesla/128 MHz	9.2 (72%)	3.0	2.5	2.6
9	3 Tesla/128 MHz	9.2 (72%)	0.2	2.7	2.9
10	3 Tesla/128 MHz	6.8 (50%)	3	2.3	2.4
11	3 Tesla/128 MHz	6.8 (50%)	0.2	2.4	2.5

+3, strong torque, the device showed rapid and forceful alignment to the magnetic field; +4, very strong torque, the device showed both very rapid and forceful alignment to the magnetic field (22–26,28–33).

MRI-Related Heating

MRI-related heating tests were conducted on different lengths of the lead fragment in order to assess those that would cause the highest temperature rises (Table 1). Thus, the lengths of the fragmented leads were selected based on findings from prior MRI testing experience with other leads, computer simulations of similar metallic objects, and information in the medical literature with respect to which length versions would create the greatest amount of heating at the frequencies of 64 MHz (1.5 Tesla) and 128 MHz (3 Tesla MR system) (21,22). The proximal ends of the leads were pulled straight and stripped of insulation to represent the shortest and longest credible cases (2 mm and 3 cm) consistent with the fragments that have occurred with the clinical use of this particular PNS lead (Unpublished observations, SPR Therapeutics). Each lead fragment was assessed according to information from the American Society for Testing Materials (ASTM) International and the peer-reviewed literature (22–24,26–34). Because implant heating associated with radiofrequency (RF) energy may be different for a given lead fragment length in relation to the transmit frequency used by the MR system (21,22), MRI-related heating was evaluated for the different lead fragments at 1.5 Tesla/64 MHz and 3 Tesla/128 MHz.

The MRI-related heating test used a plastic ASTM International phantom filled to a depth of 10 cm with a semisolid, gelled-saline (i.e., 1.32 g/L NaCl plus 10 g/L polyacrylic acid in distilled water) (22–24,26–34). Each lead fragment was placed in a position in the phantom where there was a high uniform electric field tangential to each lead fragment, ensuring extreme RF heating conditions for this experimental setup, as previously described (i.e., in consideration of an analysis of the ASTM International phantom and the MRI conditions used for this assessment) (22–24,26–34). A relatively high level of RF energy was applied under each MRI condition during the MRI-related heating evaluations (22–24,26–34). Because there is no blood flow or perfusion simulated with this experimental set up, it represents an extreme condition used to assess the various heating scenarios for the lead fragments.

MRI Conditions

MRI was performed at 1.5 Tesla/64 MHz (Magnetom, Software Numaris/4, Version Syngo MR 2002B DHHS, Siemens Medical Solutions, Malvern, PA, USA) and 3 Tesla/128 MHz (Excite, Software 14X.M5, General Electric Healthcare, Milwaukee, WI, USA). The RF body transmit coil was used in each case. The MRI parameters were selected to generate a high level of RF energy (22–24,26–34). The landmark position for both MRI system conditions was at the center of the thorax (the center of each lead fragment) of the head/torso ASTM International phantom, with multiple section locations obtained through the lead fragment. An MR system reported, whole body averaged, specific absorption rate (SAR) of 2.7 W/kg (calorimetry value, 2.1 W/kg) was used at 1.5 Tesla/64 MHz and 2.9 W/kg (calorimetry value, 2.7 W/kg) was used at 3 Tesla/128MHz, for a total imaging time of 15 min in each case.

Measurement of Temperature

Temperature recordings were obtained using a Luxtron Model 3100 Fluoroptic Thermometry System (Lumasense, Santa Clara, CA, USA) previously demonstrated to be MRI-compatible and unperturbed at static magnetic field strengths up to 9.0 Tesla (i.e., an MR spectrometer) (22–24,28–34). This thermometry system has small fiber-optic probes (Model SFF-2; 0.5 mm diameter) that respond rapidly (response time, 0.25 sec; sensitive volume radius, less than 1 mm), with an accuracy and resolution of +0.1°C. The thermometry system was calibrated immediately before obtaining temperature measurements for each experimental condition. Each lead fragment had thermometry probes attached to record representative temperatures during the heating tests, as follows: Probe #1, sensor portion of the probe placed in contact with one end of the lead fragment, uninsulated end; Probe #2, sensor portion of the probe placed in contact with opposite end of the lead fragment, tip. In addition, a thermometry probe was placed in the phantom at a position removed (at least 30 cm away from the lead and 1 cm from the opposite edge of the phantom) from the lead but within the area of MR imaging, to record a reference temperature during the heating experiment (Probe #3).

MRI-Related Heating Protocol

The gelled-saline-filled ASTM International head/torso phantom was placed in the 1.5 Tesla/64 MHz and then the 3 Tesla MR systems, respectively, and allowed to equilibrate to the environmental conditions for more than 24 hours in each case. The room temperature and temperature of the bore of each MR system were measured 15 min before and 15 min after each test session to ensure that no change greater than 0.2°C occurred. The fan for each MR system was not on during the heating tests. There was

Table 2. Summary of MRI Artifacts (Signal Loss) at 3 Tesla for the Lead Fragment (12.7 cm Length With 0.2 cm, Proximal Uninsulated End).

Pulse sequence	T1-SE	T1-SE	GRE	GRE
Signal void size (mm^2)	667	12	1197	38
Imaging plane	Parallel (long axis)	Perpendicular (short axis)	Parallel (long axis)	Perpendicular (short axis)

T1-SE, T1-weighted spin echo; GRE, gradient echo.

sufficient thermal equilibrium in the phantom such that the temperature did not change by more than 0.2°C during the pre-MRI observation time for a period of 15 min. Baseline (pre-MRI) temperatures were recorded at 4 sec. intervals for 5 min. MRI was then performed for 15 min with temperatures recorded at 4 sec intervals. Post-MRI temperatures were recorded for 2 min with temperatures recorded at 4 sec intervals. The highest temperature changes are reported, herein, for the lead fragments tested at 1.5 Tesla/64 MHz and 3 Tesla/128 MHz.

Background temperatures (i.e., heating of the phantom without each lead fragment present) were also recorded during the MRI-related heating evaluation. Accordingly, the temperature changes were measured at the same fluoroptic thermometry probe positions and at the same time intervals as those used when measuring the temperatures for each lead fragment in the gelled-saline-filled ASTM International phantom (22–24,26–34). The highest background temperature rises obtained from these assessments at 1.5 Tesla/64 MHz and 3 Tesla/128 MHz are also reported.

Artifacts

MR imaging artifacts were assessed for the lead fragment, 12.7 cm length with the proximal 2 mm, uninsulated in association with the use of a 3 Tesla MR system. MR imaging was conducted with the lead placed inside of the gadolinium-doped, saline filled, plastic phantom (15 × 15 × 24 cm) (22–24,28–33). The lead fragment was attached to a plastic frame using non-conducting, non-insulating paper tape (3M Company, Minneapolis, MN, USA) to facilitate positioning and MR imaging within this phantom. MR imaging was performed using a 3 Tesla MR system (Excite, Software 14X.M5, General Electric Healthcare, Milwaukee, WI, USA), a send–receive RF coil, and the following pulse sequences: T1-weighted, spin echo pulse sequence; repetition time, 500 msec; echo time, 20 msec; matrix size, 256 X 256; section thickness, 5 mm; field of view, 24 cm; number of excitations, 2; bandwidth; 32 kHz, and gradient echo (GRE) pulse sequence; repetition time, 100 msec; echo time, 15 msec; flip angle, 30°; matrix size, 256 × 256; section thickness, 5 mm; field of view, 24 cm; number of excitations, 2; bandwidth, 32 kHz (22–24,26–34).

Planimetry software provided with the MR system was used to measure the cross-sectional areas for the artifacts (i.e., the signal loss) associated with the lead fragment (22–24,26–34). The accuracy of this measurement method is ±10%. Measurements were obtained to determine the maximum or worst case artifact area related to the presence of the lead fragment for each MR imaging condition. This ensured that the sizes of the artifacts for the lead fragment were not underestimated. Image display parameters (i.e., window and level settings, magnification, etc.) were carefully selected and applied in a consistent manner to obtain accurate measurements of sizes for the artifacts (22–24,26–34). The 3 Tesla/128 MHz MR system was selected for the artifact assessment for the lead fragment because it represents the highest static magnetic field strength used in the clinical setting.

RESULTS

Translational attraction for the longest lead fragment (12.7 cm) was a mean deflection angle of 7° ± 0° and the qualitatively determined torque was 0, no torque at 3 Tesla.

Table 1 summarizes the results of the findings for MRI-related heating. At 1.5 Tesla/64 MHz, the highest temperature rises occurred at the uninsulated ends of the lead fragments and ranged from 2.8°C to 3.5°C. The highest background temperature rise at 1.5 Tesla/64 MHz was ≤1.5°C. At 3 Tesla/128 MHz, the highest temperature rises also occurred at the uninsulated ends of the lead fragments and ranged 2.3°C to 5.9°C. The highest background temperature rise at 3 Tesla/128 MHz was ≤1.6°C.

Artifact test results are presented in Table 2. The artifacts appeared as localized signal voids that corresponded to the size and shape of this lead fragment. The GRE pulse sequence produced larger artifacts than the T1-weighted, spin echo pulse sequence. The maximum artifact size observed on MR images obtained using the GRE pulse sequence (i.e., worst case for artifacts) extended 7 mm relative to the size and shape of the lead fragment (Fig. 4).

Figure 4. Artifact observed on MRI using a gradient echo pulse sequence. Note that the signal loss extended a maximum of 7 mm relative to the lead fragment.

DISCUSSION

Percutaneous PNS is a non-opioid, minimally invasive therapy for the treatment of pain that avoids many of the limitations of traditional permanent implantable neurostimulation modalities. This therapy has been evaluated in clinical trials encompassing multiple pain indications including low back pain, neuropathic pain following amputation, chronic shoulder pain, and postoperative pain following total knee arthroplasty (1,2,9–20). In each of these studies, a majority (60–100%) of subjects reported at least a 50% reduction in pain or pain interference at the end of the short-term ($\leq$60 day) therapy (1,9–20). Also, multiple studies have demonstrated lasting pain relief following the end of therapy (1,2,9,11–18) with one study reporting sustained clinically significant pain relief in more than 75% of subjects one year following completion of therapy (1).

The safety profile of the open-coil percutaneous lead is well-documented (35,36). Importantly, there are relatively few complications associated with percutaneous PNS, with the most commonly reported adverse events being minor skin conditions (e.g., irritation, erythema, blister, mild skin tear) that were usually attributed to the use of medical/surgical adhesive tapes, bandages, or the surface return electrode (a patch electrode with a hydrogel layer that conducts electricity and adheres to the skin) (1,2,9–20). No serious device-related adverse events have occurred across all studies and, for the adverse events that did occur, these required little or no medical treatment (1,2,9–20). In addition, there have been no reports of induced sensory, motor, or proprioception deficits during use of this unique means of applying PNS, thus, enabling percutaneous PNS to be utilized during physical rehabilitation (e.g., during the immediate postoperative period) and activities of daily living (1,2,9–20).

Infection is often one of the greatest limiting factors when using any type of percutaneous device (e.g., central venous lines). Fortunately, the risk of a clinically relevant infection reported for the lead evaluated in the present investigation is considerably lower than that for percutaneously inserted catheters used to deliver perineural local anesthetic for postoperative analgesia (e.g., continuous peripheral nerve block catheters). That is, 0.03 infections per 1000 indwelling days in the case of this percutaneously inserted lead, making the risk of infection for this medical device extraordinarily low (36).

In addition, a patient with the percutaneous PNS system who needs an MRI procedure faces fewer challenges than with traditional implantable neurostimulation systems. The use of MRI in patients with implantable neurostimulation systems is often prohibited or limited because of labeling restrictions required to prevent hazards related to magnetic field interactions, MRI-related heating, and potential damage to the implanted pulse generator (14,37). To date, a limited number of neurostimulation systems exist with labeling that permits the use of MRI examinations in patients with these active devices (14,37). In contrast, percutaneous PNS is a temporary therapy, and, therefore, the lead can be removed prior to MRI and reinserted in the same location (9–20). Furthermore, if the diagnostic study is not urgent, then MRI may be delayed until after the lead is removed at the end of the short-term therapy. Patients with leads removed intact (i.e., without retained lead fragments) have no risk of MRI-related issues from the stimulation system since none of the system components remains in the body at the end of therapy.

Removal of the lead is conducted by pulling on the exposed end, retracting the lead through the exit site along the same line in which it was implanted (1,2,9–20). The lead may fracture during lead removal, resulting in a retained metallic fragment. Accordingly, the medical professional should inform the patient regarding these matters and make a notation in the patient's medical records. It should be noted that the rate of lead fracture (as determined by visual inspection of the removed lead) associated with lead removal has been reported to be 7.5% (1,2,9–20). Notably, there were no reports of infectious or neurologic complications related to the presence of lead fragments *in situ*, nor any reports of indwelling leads fracturing during therapy (1,2,9–20). The focus of the present investigation was to determine possible issues for the patient with retained lead fragments relative to the use of MRI performed at 1.5 Tesla/64 MHz and 3 Tesla/128 MHz.

Magnetic Field Interactions

Although translational attraction and torque acting on a metallic implant may pose a risk for a patient undergoing MRI due to movement or dislodgment of the item (21,37), the lead fragments in the present study produced only minor field interactions. In this study, the largest lead fragment that was assessed for magnetic field interactions at 3 Tesla displayed a 7° deflection angle and no torque. The criterion stated by the ASTM International indicates that if the implant deflects less than 45°, then the magnetically induced deflection force is less than the force on the implant due to gravity such as those imposed by normal daily activities in the Earth's gravitational field (25). The absence of magnetic field-related issues is due to the material used to make this particular lead (MicroLead, 316L stainless steel), which has low, magnetic susceptibility. Therefore, from a magnetic field interaction consideration, a patient with any length of a retained lead fragment from this medical product will not be harmed in association with the use of a 3 Tesla or less MR system.

MRI-Related Heating

MRI-related heating that potentially results in burn injuries to patients is a risk for neurostimulation systems (21,37). In the present study, under relatively high RF power conditions at 1.5 Tesla/64 MHz and 3 Tesla/128 MHz, MRI-related heating evaluated for a wide range of lead fragment lengths demonstrated highest temperature rises of 3.5°C and 5.9°C, respectively, with the highest background temperature rises being 1.5°C and 1.6°C, respectively. MR Conditional labeling that is applied to implants extrapolates the worst-case temperature finding from the MRI-related heating test in consideration of the calorimetry determined SAR value, to the Normal Operating Mode of operation for the MR scanner (default value, whole body averaged SAR, 2 W/kg) (21,37). For example, the maximum temperature rise that would be indicated in the labeling for the lead fragment would be $\leq$3.3°C in association with 1.5 Tesla/64 MHz MRI conditions. Thus, at 1.5 Tesla/64 MHz, this worst-case temperature rise that can occur for a lead fragment during MRI will not harm the patient, especially when considering that the surrounding tissue temperatures where the lead fragment may be located (i.e., peripheral, relatively superficial tissue) is substantially less than deep body temperature (i.e., 37°C) (38–40). By comparison, the higher temperature rises observed at 3 Tesla/128 MHz conditions are potentially worrisome and, thus, warrant additional investigation that should entail a higher level of analysis to include MRI simulations using human modeling or other similar strategy. However, in the event that it is necessary to perform an MRI at 3 Tesla on a patient with a lead fragment length that may pose an issue related to excessive MRI-related heating (i.e., a lead fragment length that is 11.2–12.7 cm), the whole body averaged SAR may be reduced by adjusting the MRI pulse sequence parameters to achieve a whole

body averaged SAR value of 1 W/kg, which will result in a 50% decrease in the temperature rise and, thus, reduce the risk of the MRI examination.

Artifacts

The artifacts that were observed on the 3 Tesla, MR images related to the largest lead fragment appeared as areas of localized, signal losses in relation to the size and shape of this object, with the GRE pulse sequence exhibiting a greater area of signal loss compared with the T1-weighted, spin echo pulse sequence. Importantly, the signal loss extended approximately 7 mm from the lead fragment on the GRE pulse sequence, indicating that anatomy located at positions further than this distance may be easily visualized on MRI examinations. The investigators understand that there are a myriad of possible MRI parameters that may be utilized to characterize artifacts for metallic implants, however, the methodology used in the present investigation has been applied in many prior reports, which permits comparison to other medical devices that have undergone similar artifact assessments (21–24,26–33). It should be noted that, when patients have metallic objects present in the area of interest, parameters can be optimized to substantially reduce the associated signal loss that may impact the diagnostic use of MRI (21,22,37). Furthermore, MRI performed at lower field strengths (i.e., 1.5 Tesla and less) will inherently result in smaller artifacts for the lead fragment (21).

CONCLUSIONS

In consideration of the findings obtained from tests performed to assess magnetic field interactions, MRI-related heating, and artifacts for various lengths of lead fragments for this particular percutaneous PNS product (MicroLead), and taking into consideration conservative advice to ensure MRI safety for patients, as well as based on the current MRI labeling terminology (21,41), these lead fragments are "MR Conditional" at 1.5 Tesla, only, meaning that they have been demonstrated to pose no known hazards in a specified MRI environment with specified conditions of use indicated. Accordingly, the conditions of use to ensure patient safety include the following: 1) 1.5 Tesla only and 2) whole body averaged SAR of 2 W/kg (i.e., with the MR system operating in the Normal Operating Mode) for 15 min of scanning per pulse sequence. As a result, patients with retained lead fragments requiring MRI exams are not expected to be markedly affected since the majority of MR systems that exit worldwide operate at 1.5 Tesla/64 MHz. Notably, the results demonstrated that, even if the entire lead fragment (i.e., from the exit site at the skin to the distal tip) remains in the patient due to a fracture just below the level of the skin, this metallic object does not require total removal because of the relative lack of risks.

Authorship Statements

Frank G. Shellock, PhD provided substantial contributions to acquisition of data, analysis and interpretation of data, drafting and reviewing the manuscript for critically for important intellectual content, and final approval of the version to be published. Armaan Zare provided substantial contributions to drafting and reviewing the manuscript for critically for important intellectual content, and final approval of the version to be published. Brian M. Ilfeld, MD, MS provided substantial contributions to the conception of the study, to drafting and reviewing the manuscript critically for important intellectual content, and final approval of the version to be published. John Chae, MD, ME provided substantial contributions to the conception of the study, to drafting and reviewing the manuscript critically for important intellectual content, and final approval of the version to be published. Robert B. Strother provided substantial contributions to conception and design, analysis and interpretation of data, drafting and reviewing the manuscript for critically for important intellectual content, and final approval of the version to be published.

How to Cite this Article:

Shellock F.G., Zare A., Ilfeld B.M., Chae J., Strother R.B. 2017. *In Vitro* Magnetic Resonance Imaging Evaluation of Fragmented, Open-Coil, Percutaneous Peripheral Nerve Stimulation Leads.
Neuromodulation 2017; E-pub ahead of print. DOI:10.1111/ner.12705

REFERENCES

1. Chae J, Yu DT, Walker ME et al. Intramuscular electrical stimulation for hemiplegic shoulder pain: a 12-month follow-up of a multiple-center, randomized clinical trial. *Am J Phys Med Rehabil* 2005;84:832–842.
2. Kapural L, Gilmore CA, Chae J et al. Percutaneous peripheral nerve stimulation for the treatment of chronic low back pain: two clinical case reports of sustained rain relief. *Pain Pract* 2016;17:753–762.
3. Kumar K, Taylor RS, Jacques L et al. Spinal cord stimulation versus conventional medical management for neuropathic pain: a multicentre randomised controlled trial in patients with failed back surgery syndrome. *Pain* 2007;132:179–188.
4. Deer T, Kim C, Bowman R, Ranson M, Douglas CS, Tolentino W. Spinal cord stimulation as a method of reducing opioids in severe chronic pain: a case report and review of the literature. *W V Med J* 2010;106:56–59.
5. North RB, Kidd DH, Farrokhi F, Piantadosi SA. Spinal cord stimulation versus repeated lumbosacral spine surgery for chronic pain: a randomized, controlled trial. *Neurosurgery* 2005;56:98–107.
6. Cameron T. Safety and efficacy of spinal cord stimulation for the treatment of chronic pain: a 20-year literature review. *J Neurosurg* 2004;100:254–267.
7. Taylor RS, Van Buyten J-P, Buchser E. Spinal cord stimulation for chronic back and leg pain and failed back surgery syndrome: a systematic review and analysis of prognostic factors. *Spine* 2005;30:152–160.
8. Sharan AD, Riley J, Falowski SM et al. Association of opioid usage with spinal cord stimulation outcomes. Presented at North American Neuromodulation Society 20th Annual Meeting 2017, Las Vegas, NV.
9. Rauck RL, Cohen SP, Gilmore CA et al. Treatment of post-amputation pain with peripheral nerve stimulation. *Neuromodulation* 2014;17:188–197.
10. Rauck RL, Kapural L, Cohen SP et al. Peripheral nerve stimulation for the treatment of postamputation pain. A case report. *Pain Pract* 2012;12:649–655.
11. Renzenbrink GJ, IJzerman MJ. Percutaneous neuromuscular electrical stimulation (P-NMES) for treating shoulder pain in chronic hemiplegia. Effects on shoulder pain and quality of life. *Clin Rehabil* 2004;18:359–365.
12. Yu DT, Chae J, Walker ME, Hart RL, Petroski GF. Comparing stimulation-induced pain during percutaneous (intramuscular) and transcutaneous neuromuscular electric stimulation for treating shoulder subluxation in hemiplegia. *Arch Phys Med Rehabil* 2001;82:756–760.
13. Chae J, Wilson RD, Bennett ME, Lechman TE, Stager KW. Single-lead percutaneous peripheral nerve stimulation for the treatment of hemiplegic shoulder pain: a case series. *Pain Pract* 2013;13:59–67.
14. Wilson RD, Bennett ME, Lechman TE, Stager KW, Chae J. Single-lead percutaneous peripheral nerve stimulation for the treatment of hemiplegic shoulder pain: a case report. *Arch Phys Med Rehabil* 2011;92:837–840.
15. Wilson RD, Harris MA, Bennett ME, Chae J. Single-lead percutaneous peripheral nerve stimulation for the treatment of shoulder pain from subacromial impingement syndrome. *PM R* 2012;4:624–628.
16. Yu DT, Chae J, Walker ME et al. Intramuscular neuromuscular electric stimulation for poststroke shoulder pain: a multicenter randomized clinical trial. *Arch Phys Med Rehabil* 2004;85:695–704.
17. Wilson RD, Gunzler DD, Bennett ME, Chae J. Peripheral nerve stimulation compared with usual care for pain relief of hemiplegic shoulder pain: a randomized controlled trial. *Am J Phys Med Rehabil* 2014;93:17–28.
18. Wilson RD, Harris MA, Gunzler DD, Bennett ME, Chae J. Percutaneous peripheral nerve stimulation for chronic pain in subacromial impingement syndrome: a case series. *Neuromodulation* 2014;17:771–776.

19. Ilfeld BM, Grant SA, Gilmore CA et al. Neurostimulation for post-surgical analgesia: a novel system enabling ultrasound-guided percutaneous peripheral nerve stimulation. *Pain Pract* 2017;17:892–901.
20. Ilfeld BM, Gilmore CA, Grant SA et al. Ultrasound-guided percutaneous peripheral nerve stimulation for analgesia following total knee arthroplasty: a prospective feasibility study. *J Orthop Surg Res* 2017;12:4.
21. Shellock FG. *Reference manual for magnetic resonance safety, implants, and devices*, 2017 ed. Los Angeles, CA: Biomedical Research Publishing Group, 2017.
22. Shellock FG, Audet-Griffin A. Evaluation of magnetic resonance imaging issues for a wirelessly-powered lead used for epidural, spinal cord stimulation. *Neuromodulation* 2014;17:334–339.
23. Shellock FG, Knebel J, Prat A. Evaluation of MRI issues for a new neurological implant, the Sensor Reservoir. *Magn Reson Imaging* 2013;31:1245–1250.
24. Weiland JD, Faraji B, Greenberg RJ, Humayun MS, Shellock FG. Assessment of MRI issues for the Argus II retinal prosthesis. *Magn Reson Imaging* 2012;30:382–389.
25. ASTM International: F2052. Standard test method for measurement of magnetically induced displacement force on passive implants in the magnetic resonance environment. In: *Annual book of ASTM standards: medical devices*, Vol. 13.01. West Conshohocken, PA: American Society for Testing and Materials, 2002:1576–1580.
26. Shellock FG, Valencerina S. In vitro evaluation of MR imaging issues at 3-T for aneurysm clips made from MP35N: findings and information applied to 155 additional aneurysm clips. *AJNR Am J Neuroradiol* 2010;31:615–619.
27. Shellock FG, Kanal E, Gilk T. Confusion regarding the value reported for the term "spatial gradient magnetic field" and how this information is applied to labeling of medical implants and devices. *AJR Am J Roentgenol* 2011;196:142–145.
28. Karacozoff AM, Shellock FG. Fiducial marker for lung lesion: *in vitro* assessment of MRI issues at 3-Tesla. *AJR Am J Roentgenol* 2013;200:1234–1237.
29. Gill A, Shellock FG. Assessment of MRI issues at 3-Tesla for metallic surgical Implants: findings applied to 61 additional skin closure staples and vessel Ligation clips. *J Cardiovasc Magn Reson* 2012;14:3.
30. Karacozoff AM, Shellock FG, Wakhloo AK. A next-generation, flow-diverting implant used to treat brain aneurysms: in vitro evaluation of magnetic field interactions, heating and artifacts at 3-T. *Magn Reson Imaging* 2013;31:145–149.
31. Titterington B, Puschmann C, Shellock FG. A new vascular coupling device: assessment of MRI issues at 3-Tesla. *Magn Reson Imaging* 2014;32:585–589.
32. Shellock FG, Giangarra CJ. *In vitro* assessment of 3-T MRI issues for a bioabsorbable, coronary artery scaffold with metallic markers. *Magn Reson Imaging* 2014; 32:163–167.
33. Titterington B, Shellock FG. Evaluation of MRI issues for an access port with a radiofrequency identification (RFID) tag. *Magn Reson Imaging* 2013;31: 1439–1444.
34. American Society for Testing and Materials International, Designation F 2182-011a. *Standard test method for measurement of radio frequency induced heating near passive implants during magnetic resonance imaging*. West Conshohocken, PA: ASTM International, 2011.
35. Knutson JS, Naples GG, Peckham PH, Keith MW. Electrode fracture rates and occurrences of infection and granuloma associated with percutaneous intramuscular electrodes in upper-limb functional electrical stimulation applications. *J Rehabil Res Dev* 2002;39:671–683.
36. Ilfeld BM, Gabriel RA, Saulino MF et al. Infection rates of electrical leads used for percutaneous neurostimulation of the peripheral nervous system. *Pain Pract* 2016;6: 753–762.
37. Shellock FG. MRI safety and neuromodulation systems. In: Krames ES, Peckham PH, Rezai AR, eds. *Neuromodulation*. New York: Academic Press, 2009: 243–281.
38. van Rhoon GC, Samaras T, Yarmolenko PS, Dewhirst MW, Neufeld E, Kuster N. CEM43°C thermal dose thresholds: a potential guide for magnetic resonance radiofrequency exposure levels?. *Eur Radiol* 2013;23:2215–2227.
39. Dewhirst MW, Viglianti BL, Lora-Michiels M, Hoopes PJ, Hanson M. Thermal dose requirement for tissue effect: experimental and clinical findings. *Proc SPIE Int Soc Opt Eng* 2003;2:37.
40. Webb P. Temperatures of skin, subcutaneous tissue, muscle and core in resting men in cold, comfortable and hot conditions. *Eur J Appl Physiol Occup Physiol* 1992; 64:471–476.
41. Shellock FG, Woods TO, Crues JV. MR labeling information for implants and devices: explanation of terminology. *Radiology* 2009;253:26–30.

